



## Optical Beam Steering Based on the Symmetry of Resonant Modes of Nanoparticles

Junjie Du,<sup>1,\*</sup> Zhifang Lin,<sup>2,3</sup> S. T. Chui,<sup>4,†</sup> Wanli Lu,<sup>2,3</sup> Hao Li,<sup>1</sup> Aimin Wu,<sup>1</sup> Zhen Sheng,<sup>1</sup> Jian Zi,<sup>2,3</sup> Xi Wang,<sup>1</sup> Shichang Zou,<sup>1</sup> and Fuwan Gan<sup>1,‡</sup>

<sup>1</sup>State Key Laboratory of Functional Materials for Informatics, Institute of Microsystem and Information Technology, Chinese Academy of Sciences, Shanghai 200050, China

<sup>2</sup>State Key Laboratory of Surface Physics and Department of Physics, Fudan University, Shanghai 200433, China

<sup>3</sup>Key Laboratory of Micro and Nano Photonic Structures (Ministry of Education), Fudan University, Shanghai, China

<sup>4</sup>Bartol Research Institute, University of Delaware, Newark, Delaware 19716, USA

(Received 21 March 2011; revised manuscript received 27 April 2011; published 20 May 2011)

We report a phenomenon that an optical beam transmits in a negative direction when passing through a single array of high-refractive-index dielectric nanorods. The mechanism of the negative directional transmission is believed to be due to the symmetry of resonant modes in the dielectric nanoparticles. It is expected to find applications in designing compact optical components to achieve the on-chip beam steering in photonic circuits.

DOI: 10.1103/PhysRevLett.106.203903

PACS numbers: 41.20.Jb, 42.25.Fx, 73.20.Mf, 78.20.Ci

Resonance, in particular, subwavelength resonance where resonant wavelength is much larger than the size of resonator, plays an important role in many fields of physics. Subwavelength resonant units have indeed become the basic building blocks in artificially structured electromagnetic (EM) materials. Particles with different resonant properties assume different functions in manipulating EM waves. For instance, the localized surface plasmon resonance of noble metal particles enables guiding of the EM energy below the diffraction limit [1]. The magnetic resonance of a split ring provides an effective negative magnetic permeability [2], which, when combined with metallic rods, leads to the implementation of the negative-refractive-index materials [3]. The subwavelength resonant units in metamaterials also offer an approach to achieve seemingly arbitrary effective permittivity and permeability, leading to many interesting phenomena, which, among others, include invisibility cloaking [4], optical illusion [5], and the photonic analog of the black hole [6]. By carefully tuning the resonances in multiple angular momentum channels (AMCs) [7] of nanoparticles to a nearly degenerate frequency, one is able to beat the single channel limit of total scattering cross section, giving rise to a superscattering effect [8].

While most subwavelength resonators were based upon metallic components taking advantage of the plasmonic resonance, dielectric particles with high electric permittivity (high  $\epsilon$ ) also show the unique property of supporting subwavelength resonance in the lower AMCs. Therefore, they offer an alternative way to produce the negative refraction behavior [9] and transfer EM energy below the diffraction limit [10], with the potential for operation at near optical frequencies with lower absorption loss in comparison with their metallic counterpart.

Up to now, much effort concerning the subwavelength resonance in the EM community has been devoted to

producing the desired permittivity and permeability, while the symmetry nature of the resonance in different AMCs, together with its physical consequence in manipulating EM waves, remains far less explored. The only two examples we are aware of are the observation of a finite circulation in the reflected beam [11] and the unidirectional EM edge states [12] because of the broken time reversal symmetry of the scatterer in a magnetic field. In this Letter, we report another interesting phenomenon in which the incident beam can be manipulated with the symmetry of resonant modes inside high- $\epsilon$  dielectric nanoparticles. As a result, when an optical beam strikes on an array of high- $\epsilon$  dielectric nanorods, the outgoing beam can propagate in a “negative” direction as shown in Fig. 1(d); namely, the outgoing (transmitted) beam makes a sharp turn and lies on the same side of the normal as the incident beam. Unlike another interesting phenomenon of negative refraction [3], which guides the refracted beam to travel in a negative way in another effective material, the negative directional transmitted beam studied here lies in the same medium as the incident beam after passing through a single array of nanoparticles. Therefore, it may serve as an optical component for beam steering in the chip-to-chip interconnect systems and on-chip architecture. It is noted that one way to steer light by a magnetic field was proposed based on the photonic Hall effect [13]. Recently, a series of important progress has been made toward the on-chip beam steering, including the use of the photonic crystal [14], nano-Yagi-Uda antenna [15], and flat dielectric gratings [16]. Because of the ultracompact characteristic and the extremely low absorption loss feature in the dielectric system, our structure may provide yet another alternative approach to gain a high degree of on-chip control over the flow of optical beams for optical circuit.

Let us start by studying the properties of resonant states in the lowest two AMCs for a single particle. For simplicity,

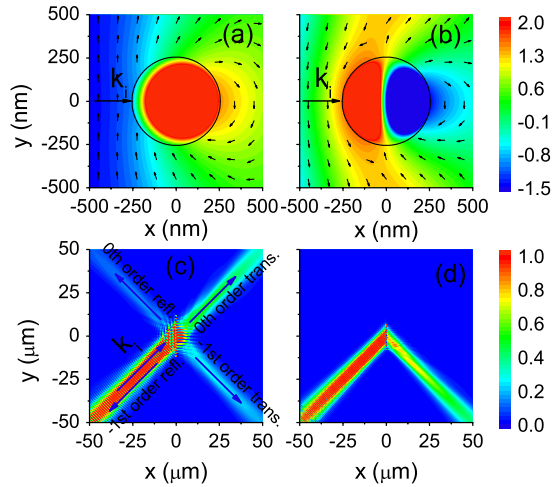


FIG. 1 (color online). The  $H$  field distribution at the resonance in the 0th (a) and 1st (b) AMCs, corresponding to  $\lambda = 2362$  and  $1550$  nm, respectively, for a single Si nanorod of radius  $r_s = 255$  nm. The black arrows display the direction of the  $E$  field on the mesh points at regular intervals outside the rod. Distribution of  $H$  field intensity when a Gaussian beam strikes a single-layer array in the  $y$  direction composed of 15 Si nanorods at frequencies corresponding to the resonance in the 0th (c) and 1st (d) AMCs. The arrows in (c) display the direction of four different Bragg diffracted orders.

we consider the two-dimensional case where the field is uniform in the  $z$  direction and the  $H$  field is polarized along  $z$ . Take silicon as an example of high- $\epsilon$  dielectric. In the optical frequency region we are interested in, the real part of its permittivity is 12.0 and the imaginary part negligible [17]. Figures 1(a) and 1(b) show that the magnetic ( $H$ ) field pattern exhibits the isotropic symmetry at resonance in the 0th AMC, corresponding to incident wavelength  $\lambda = 2362$  nm, and the dipole symmetry at resonance in the 1st AMC corresponding to  $\lambda = 1550$  nm, for a single nanorod with radius  $r_s = 255$  nm.

When the particles are arrayed in a line, the symmetry of the resonant modes of different AMCs in individual particles determines the direction of the outgoing beams. At a wavelength  $\lambda = 2362$  nm, corresponding to the 0th order AMC resonance, Fig. 1(c) shows that there appear four outgoing Bragg beams, in concert with the isotropic symmetry of resonant mode in the 0th AMC. For the 1st AMC resonance at a wavelength  $1550$  nm, the dipole symmetry completely suppresses the conventional (0th order) transmitted and reflected Bragg beams, leaving us with only one transmitted beam propagating in the negative direction, as shown in Fig. 1(d). Here the separation between adjacent rods is  $a_0 = \lambda/\sqrt{2}$ . Such an array functions as a grating which only supports the 0th and  $-1$ st diffraction orders when the angle of incidence is  $\theta_i = 45^\circ$  [18]. The higher order reflection is usually enhanced by blazed gratings. Recently, some efforts have been made to enhance the  $-1$ st order transmission for soft-x-ray band using the total external reflection [19]. We demonstrate here that the

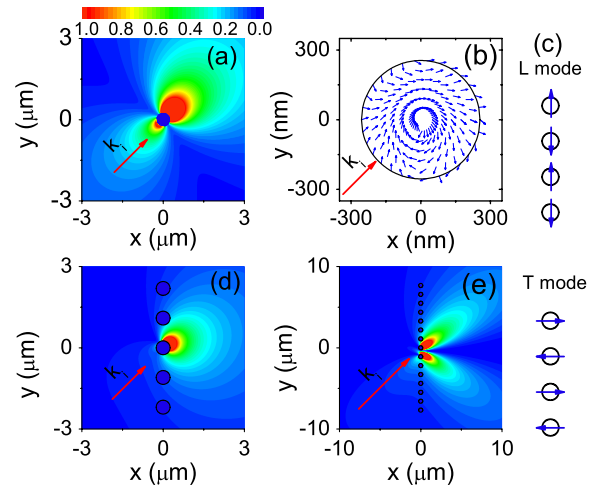


FIG. 2 (color online). (a) The scattered  $H$  field intensity of an isolated rod at the 1st AMC resonance. (b) The time-averaged Poynting vector inside a rod located in the array, showing a vortex of energy flow and implying a rotating dipole excited in the rod. (c) The longitudinal mode and transverse mode, with the excited dipole aligned along and normal to the linear array, respectively. (d) The scattered  $H$  field intensity from one rod located in the array. (e) The scattered  $H$  field intensity from a pair of adjacent rods in the array. The presence of many rods in (d) and (e) implies the interrod coupling is considered compared to the case in (a).

symmetry at the 1st AMC resonance offers another way to achieve the  $-1$ st order transmission of the beam, while drastically suppressing the zeroth order reflected and transmitted waves, with the structure much thinner than the operational wavelength.

We next illustrate the relation between the negative transmission and the dipole resonant symmetry. At the resonance in the 1st AMC, the scattered field exhibits the dipole radiation symmetry, as shown in Fig. 2(a) for a single rod. Because of this symmetry and the coupling between dipolar resonance of individual rods, the array made up of the nanorods supports two different modes: the transverse ( $T$ ) mode, with dipole moments oriented perpendicular to the chain axis, and the longitudinal ( $L$ ) mode, with dipole moments aligned with the chain axis [20,21]. The incident field excites both the  $L$  and the  $T$  modes but with a finite phase difference, resulting in a rotating dipole moment on each rod, which manifests itself by a finite vortex of energy flow, as shown in Fig. 2(b). The excited dipole on each rod in the array radiates in a strikingly different way from a dipole excited in an isolated rod, namely, the scattered field on the illumination side is substantially attenuated, as can be seen by a comparison between Figs. 2(a) and 2(d). This explains the vanishing of the conventional (zeroth order) reflected waves. In addition, as the incident wavelength  $\lambda = \sqrt{2}a_0$  and incident angle  $\theta_i = \pi/4$ , the induced dipole moments in adjacent rods have a phase difference of  $\pi$ , as schematically shown in Fig. 2(c). As a result, the scattered fields on the

transmission side from a pair of adjacent rods interfere to produce radiation mainly in 0th and  $-1$ st order transmitted directions as shown in Fig. 2(e). While the scattered field in the 0th order transmitted direction cancels out the incident field, the scattered field in the  $-1$ st order transmitted direction is left as the propagating beam in negative direction, as displayed in Fig. 1(d). It is thus concluded that the phenomenon originates from the dipole symmetry of the 1st AMC resonance of the subwavelength high- $\epsilon$  particles.

Now we proceed to a rigorous calculation of the transmissivity and reflectivity by multiple scattering theory. The nanorods are arrayed in the  $y$  direction with the  $l$ th rods located at  $\mathbf{R}_l = la_0\hat{\mathbf{e}}_y$ . The incoming and scattered  $H$  fields of rod  $l$  are expanded as  $H_i^{(l)} = \sum_n i^n p_n^{(l)} J_n(k_b r_l) e^{in\phi_l}$  and  $H_s^{(l)} = \sum_n i^n a_n^{(l)} H_n^{(1)}(k_b r_l) e^{in\phi_l}$ , where  $\mathbf{r}_l = \mathbf{r} - \mathbf{R}_l = r_l(\hat{\mathbf{e}}_x \cos\phi_l + \hat{\mathbf{e}}_y \sin\phi_l)$ ,  $p_n^{(l)} = e^{-in\theta_i} e^{i\mathbf{k}_b \cdot \mathbf{R}_l}$ ,  $J_n$  and  $H_n^{(1)}$  are, respectively, the  $n$ th order Bessel function and Hankel function of the first kind, and  $\mathbf{k}_b$  is the wave vector of the incident plane wave. The  $n$ th term in the summation denotes the  $n$ th AMC. The Mie scattering coefficient  $\alpha_n$  can be written as [7]  $\alpha_n = -1/(1 + i \cot\eta_n)$ , with  $\eta_n$  being the scattering phase shift of the  $n$ th AMC. The peaks of  $|\tan\eta_n|$  versus frequency, as shown in Fig. 3(a) for a rod with  $r_s = 255$  nm, correspond to the Mie resonance of a single rod in different AMCs [7].

By Floquet's theorem,  $a_n^{(l)} = a_n^{(0)} e^{ik_y la_0}$  with  $k_y = k_b \sin\theta_i$ . A linear set of equations can be obtained and solved for  $a_n^{(0)}$ . The reflected field is then given in terms of diffracted waves of different orders  $\nu$  as

$$H_r(r) = \sum_{\nu} r_{\nu} e^{i(k_{\nu}y - \beta_{\nu}x)}, \quad (1)$$

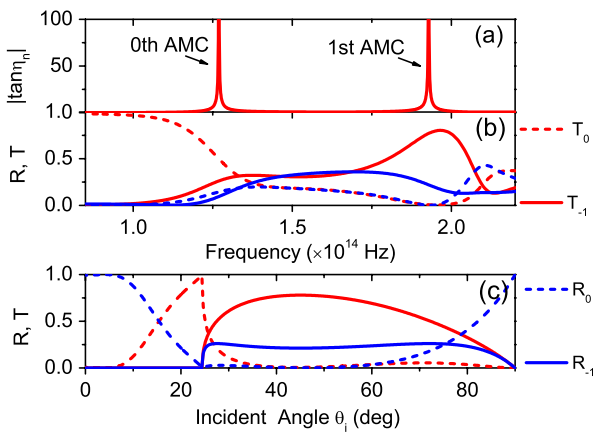


FIG. 3 (color online). (a)  $|\tan\eta_n|$  versus frequency for a single Si rod with radius  $r_s = 255$  nm. The peaks denote the 0th and 1st AMC resonances. (b) Reflectivity and transmissivity versus frequency for a linear array of rods, with  $a_0 = \lambda/\sqrt{2}$  and the incident angle  $\theta_i = 45^\circ$ . (c) Reflectivity and transmissivity versus  $\theta_i$  for a linear array of rods with  $a_0 = \lambda/\sqrt{2}$  and  $\lambda = 1550$  nm, corresponding to the 1st AMC resonance.

with

$$r_{\nu} = \frac{2}{a_0} \frac{1}{\beta_{\nu}} \sum_{n=-\infty}^{+\infty} \frac{i^n a_n^{(0)} (k_{\nu} - i\beta_{\nu})^n}{k_b^n}. \quad (2)$$

Here  $\beta_{\nu} = \sqrt{k_b^2 - k_{\nu}^2}$  for  $k_b^2 \geq k_{\nu}^2$  and  $\beta_{\nu} = i\sqrt{k_{\nu}^2 - k_b^2}$  for  $k_b^2 < k_{\nu}^2$ , with  $k_{\nu} = k_y + g_{\nu}$  and  $g_{\nu} = 2\nu\pi/a_0$ . Similarly, one has the transmitted field,

$$H_t(r) = \sum_{\nu} t_{\nu} e^{i(k_{\nu}y + \beta_{\nu}x)} \quad (3)$$

with  $t_{\nu} = t'_{\nu} + \delta_{\nu 0}$ , and

$$t'_{\nu} = \frac{2}{a_0} \frac{1}{\beta_{\nu}} \sum_{n=-\infty}^{+\infty} \frac{i^n a_n^{(0)} (k_{\nu} + i\beta_{\nu})^n}{k_b^n}. \quad (4)$$

Equations (1) and (3) show that only the 0th and  $-1$ st diffracted waves are propagating for the case with  $\lambda/a_0 = \sqrt{2}$  and  $\theta_i = 45^\circ$ . The reflectivity  $R_{\nu} = |r_{\nu}|^2$  and transmissivity  $T_{\nu} = |t_{\nu}|^2$  versus frequency for  $\nu = 0$  and  $-1$  are shown in Fig. 3(b). The effect of the resonant symmetry on the beam steering is observed by a comparison between Figs. 3(a) and 3(b). As the incident frequency approaches the resonance in the 0th AMC, the diffracted waves in the four directions tend to have nearly the same amplitude, due to the isotropic symmetry of the resonance. As the frequency goes close to the 1st AMC resonance with the dipole symmetry, our calculation shows that  $t'_0 \approx -1$ , implying that the scattered wave will cancel out the incident wave due to the destructive interference, and thus the 0th order transmitted wave vanishes. In addition, since the radiation from the rod in the array on the illumination side is dramatically attenuated, especially in the 0th order reflected direction, as shown in Fig. 2, one has  $R_0 \approx 0$  and the zeroth order reflected wave is also suppressed. The rigorous calculation corroborates our analysis about the scattering properties of the rod in the array shown in Fig. 2.

The angle resolved transmissivity (reflectivity) spectra is shown in Fig. 3(c) at frequency of the resonance in the 1st AMC. It shows that  $-1$ st order beam will be the only transmitted beam for a wide range of incident angles starting from  $30^\circ$  to  $60^\circ$  for the given structure with  $a_0 = \lambda/\sqrt{2}$  and  $\lambda = 1550$  nm, providing an acceptable angular tolerance for the beam steering.

In Fig. 4, we further show a scheme to simultaneously enhance the frequency bandwidth and the transmissivity for the negative transmission. This is done by introducing another nanorod with smaller radius in each unit cell, as shown in the inset of Fig. 4(a), where the smaller rod has radius  $r'_s = 0.4r_s$  and is placed in touch with the larger rod in each unit cell. Two touching rods form a doublet. Near the 1st AMC resonance of the larger rod, there appear two resonances, one from the larger rod itself, the other from the doublet structure. The occurrence of two resonant peaks is shown in Fig. 4(b), where the total scattering cross sections (TSCS)  $\sigma_{\text{sca}}/\pi r_s^2$  versus frequency for a single rod and the doublet structure are plotted. An enhancement of

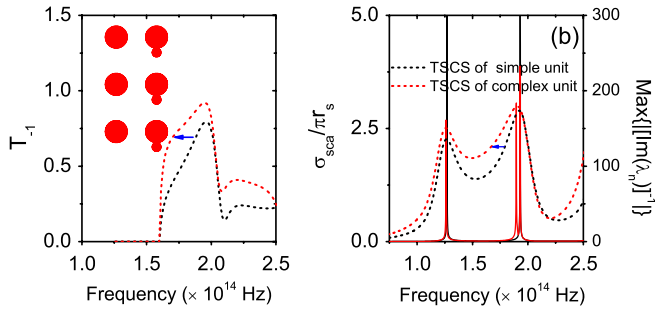


FIG. 4 (color online). (a) The transmissivity  $T_{-1}$  of the  $-1$ st order transmitted wave for the arrays made up of singlets (black dashed line) and doublets [gray (red) dashed line]. The inset shows the unit cell of the singlet and doublet. Both lattice separations are  $a_0 = 1096$  nm for the singlet and doublet structures for which the beam steering can be realized near the wavelength  $\lambda = 1550$  nm. (b) Total scattering cross section (dashed lines) and collective resonance spectrum [10] (solid lines) for singlet (black) and doublet [gray (red)] structures.

resonant bandwidth is obvious, which leads to the broadening of bandwidth for the negative transmission and thus beam steering. Another advantage of using doublet structure is that it simultaneously enhances the transmission. The  $-1$ st order transmissivity can reach 0.9, in comparison with 0.8 for array made up of single rod, as shown in Fig. 4(a).

Finally, the underlying physics for the negative transmission phenomenon suggests that it is neither limited to circular cross section of rod nor to the two-dimensional case. In Fig. 5(a), we present the field distribution near an array consisting of infinite nanorods of square cross section at the 1st AMC resonance. The length of the side of the square is 462 nm. The calculation shows that the array enables the same manipulation of beams using COMSOL MULTIPHYSICS. As an example of three dimensions, in Fig. 5(b) we show the  $H$  field intensity pattern for an array composed of 4  $\mu\text{m}$ -high rods of radius 255 nm. The calculation is carried out with the finite-difference time-domain method. The sharp turn of optical beams by the

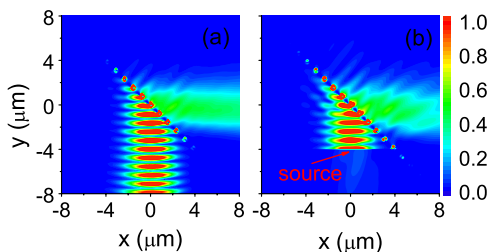


FIG. 5 (color online). Distribution of the  $H$  field intensity when a linear array composed of (a) square rods of side length 462 nm and (b) 4  $\mu\text{m}$ -high circular rods with radius 255 nm is illuminated by a Gaussian beam, demonstrating beam steering using a single array of rods with noncircular cross section and three-dimensional particles. The incident wavelength is  $\lambda = 1550$  nm for both cases.

single-layer array is again demonstrated near the dipolar resonance of individual particles.

In summary, we have shown that beam steering is possible using a single-layer array composed of high- $\epsilon$  dielectric nanorods based on the 1st AMC resonance. With the capability to operate in optical frequency at low loss, the phenomenon is expected to find applications in designing compact optical components in photonic circuits.

We would like to thank Professor C.T. Chan, Professor R.X. Wu, and Dr. S.Y. Liu for helpful discussions. This work was supported by the China-973 Program (2010CB832906, 2011CB922004), NSFC, MOE of China (B06011), SMCST (10DJ1400400, 10706200500, 08DJ1400302). S.T. Chui is partly supported by the U.S. DOE.

\*phyjunjie@gmail.com

†chui@udel.edu

‡fuwan@mail.sim.ac.cn

- [1] S. A. Maier *et al.*, *Nature Mater.* **2**, 229 (2003).
- [2] J. B. Pendry *et al.*, *IEEE Trans. Microwave Theory Tech.* **47**, 2075 (1999).
- [3] J. B. Pendry, *Phys. Rev. Lett.* **85**, 3966 (2000); R. A. Shelby *et al.*, *Science* **292**, 77 (2001).
- [4] J. B. Pendry *et al.*, *Science* **312**, 1780 (2006); U. Leonhardt, *Science* **312**, 1777 (2006); D. Schurig *et al.*, *Science* **314**, 977 (2006).
- [5] Y. Lai *et al.*, *Phys. Rev. Lett.* **102**, 253902 (2009).
- [6] D. A. Genov *et al.*, *Nature Phys.* **5**, 687 (2009); S. Y. Liu *et al.*, *Phys. Rev. B* **82**, 054204 (2010); Q. Cheng *et al.*, *New J. Phys.* **12**, 063006 (2010).
- [7] H. C. van de Hulst, *Light Scattering by Small Particles* (Dover, New York, 1981).
- [8] Z. Ruan and S. Fan, *Phys. Rev. Lett.* **105**, 013901 (2010).
- [9] J. A. Schuller *et al.*, *Phys. Rev. Lett.* **99**, 107401 (2007); L. Peng *et al.*, *Phys. Rev. Lett.* **98**, 157403 (2007); S. Y. Liu *et al.*, *Phys. Rev. Lett.* **101**, 157407 (2008); K. Vynck *et al.*, *Phys. Rev. Lett.* **102**, 133901 (2009).
- [10] J. Du *et al.*, *Phys. Rev. A* **79**, 051801(R) (2009); G. S. Blausstein *et al.*, *Opt. Express* **15**, 17380 (2007).
- [11] S. T. Chui *et al.*, *J. Phys. Condens. Matter* **22**, 182201 (2010).
- [12] F. D. M. Haldane and S. Raghu, *Phys. Rev. Lett.* **100**, 013904 (2008); Z. Wang *et al.*, *Phys. Rev. Lett.* **100**, 013905 (2008); Z. Wang *et al.*, *Nature (London)* **461**, 772 (2009); Y. Poo *et al.*, *Phys. Rev. Lett.* **106**, 093903 (2011).
- [13] D. Lacoste *et al.*, *J. Opt. Soc. Am. A* **15**, 1636 (1998).
- [14] Y. Kurosaka *et al.*, *Nat. Photon.* **4**, 447 (2010).
- [15] T. Kosako *et al.*, *Nat. Photon.* **4**, 312 (2010).
- [16] D. Fattal *et al.*, *Nat. Photon.* **4**, 466 (2010).
- [17] E. D. Palic, *Handbook of Optical Constants in Solids* (Academic, New York, 1985).
- [18] M. Mansuripur, *Classical Optics and Its Applications* (Cambridge University Press, Cambridge, England, 2002).
- [19] R. K. Heilmann *et al.*, *Opt. Express* **16**, 8658 (2008).
- [20] A. Devilez, B. Stout, and N. Bonod, *Phys. Rev. B* **81**, 245128 (2010).
- [21] K. B. Crozier *et al.*, *Opt. Express* **15**, 17482 (2007).